05,01

Ferromagnetic resonance in a single-domain particle with uniaxial anisotropy under longitudinal excitation

© T.M. Vasilevskaya, D.I. Sementsov¶, A.M. Shuty

Ulyanovsk State University,
Ulyanovsk, Russia

¶ E-mail: sementsovdi42@mail.ru

Received September 28, 2021
Revised September 28, 2021
Accepted October 10, 2021

An additional resonance peak near the effective anisotropy field H_{KN} is identified on the basis of analysis of magnetization precession dynamics of single-domain uniaxial magnetic ellipsoid particle in the spectrum of ferromagnetic resonance, corresponding to bias along the „hard" axis, under longitudinal excitation by a weak high-frequency field. This peak is related to manifestation of the angular bistability arising due-to the presence of two symmetrical angular equilibrium positions of particle magnetization in a field that is weaker than the H_{KN} field.

Key words: ferromagnetic resonance, „hard" plane, longitudinal excitation, bistability, effective anisotropy, precession trajectory, high-frequency response.

DOI: 10.21883/PSS.2022.02.54006.214

1. Introduction

Features of the dynamic behavior of dipole lattice structures are associated not only with discrete spatial ordering of nanoparticles and their interaction, but also with magnetic properties of individual particles that form the lattice. Precession dynamics of magnetic moment of an individual single-domain micro- and nano-particle depends largely on its size, symmetry, magnetic anisotropy, as well as on the value and orientation of external static and varying fields [1–8].

One of manifestations of the magnetic moment (MM) dynamics in a high-frequency field is ferromagnetic resonance (FMR) [9–11]. It is known that a uniaxial magnetic film magnetized in its plane along the „hard" axis has two resonance branches in the FMR spectrum at low frequencies with different type of the dependence of frequency on the bias field [10]. The resonance frequency tends to zero at a field value where both branches converge. According to the theory, there is no resonance peak for the finite frequency at the above-mentioned field value. However, in [12] such a peak was detected experimentally, and in [13] it was shown that the emergence of this resonance peak is related to the manifestation of angular bistability in the MM precession motion of the film.

As far as the type of main resonance dependencies is to a large extent common for specimens with different composition, geometry, anisotropy, we consider that resonance features like these can manifest in FMR spectra of individual single-domain uniaxial micro- or nano-particle and, as a consequence, in lattices formed by such particles. This work shows, on the basis of numerical solution to the Landau–Lifshitz equation and analysis of MM precession dynamics of a uniformly magnetized ellipsoid specimen, that presence of two close angular equilibrium positions under bias in the „hard" direction by a field with value close to that of the effective anisotropy field H_{KN} results in a resonance response and bistability of the MM precession even under longitudinal excitation by a weak high-frequency field (i. e. at $\mathbf{h} \parallel \mathbf{H}_0$ and $h \ll H_0$). In this case the resonance response is even stringer than that of the transverse excitation (when $\mathbf{h} \perp \mathbf{H}_0$). Also, it worth to note that with the excitation field amplitude and frequency used in this work the uniform mode is significantly distant in frequency from the spin-wave mode, thus there is no energy transfer from the uniform precession to spin waves and no development of spin-wave instabilities [14–16].

2. General relationships

Let us consider a specimen shaped as an oblong ellipsoid of revolution. We assume that, along with the shape anisotropy, the specimen has a weak induced uniaxial anisotropy, which axis of easy magnetization is coincident with the symmetry axis of the specimen. In this case the free-energy density contains Zeeman energy, anisotropy energy, and energy of scattering fields

$$F = -\mathbf{M}(\mathbf{H}_0 + \mathbf{h}) + K\sin^2\theta + \frac{1}{2}\mathbf{M}\widehat{N}\mathbf{M}. \qquad (1)$$

Here: K — constant value of the uniaxial anisotropy, θ — polar angle of vector $\mathbf{M}$ measured from the symmetry axis of the ellipsoid (OZ axis), $\widehat{N}$ — diagonal tensor with components related to each other by the following relationship: $N_x + N_y + N_z = 4\pi$ and dependent on the ratio between the longitudinal and transverse semi-axes of the ellipsoid: $n = l_{\parallel}/l_{\perp}$ [10]. For oblong ellipsoid of revolution: $n > 1$, $N_x = Ny = N_\perp$, $N_z = N_\parallel$, and

$$\Delta N = N_\perp - N_\parallel$$
$$= 2\pi \left\{ 1 - \frac{3}{n^2-1} \left[\frac{n}{\sqrt{n^2-1}} \ln\left(n+\sqrt{n^2-1}\right) - 1 \right] \right\}. \quad (2)$$

Individual components of tensor $\widehat{N}$ can be written as follows

$$N_\parallel = \frac{4\pi}{3} - \frac{2}{3}\Delta N, \quad N_\perp = \frac{4\pi}{3} + \frac{1}{3}\Delta N. \quad (3)$$

Timedependence of vector orientation and features of its precession dynamics for various cases of bias and high-frequency excitation of particle are determined on the basis of numerical solution to the Landau–Lifshitz equation written in spherical coordinates [11]:

$$\frac{\partial\theta}{\partial t} = -\frac{\gamma\alpha}{M}\frac{\partial F}{\partial\theta} - \frac{\gamma}{M\sin\theta}\frac{\partial F}{\partial\varphi},$$
$$\frac{\partial\varphi}{\partial t} = \frac{\gamma}{M\sin\theta}\frac{\partial F}{\partial\theta} - \frac{\gamma\alpha}{M\sin^2\theta}\frac{\partial F}{\partial\varphi}, \quad (4)$$

where α — dimensionless constant of attenuation, and free-energy density of the specimen is defined by relationship (1). In general, frequency of the magnetization resonance precession is defined by the following general expression:

$$\omega_{\text{res}} = \frac{\gamma}{M\sin\theta}\left[\left(\frac{\partial^2 F}{\partial\varphi^2}\right)_0\left(\frac{\partial^2 F}{\partial\theta^2}\right)_0 - \left(\frac{\partial^2 F}{\partial\varphi\partial\theta}\right)_0^2\right]^{1/2}, \quad (5)$$

where second order derivatives of the free energy are calculated for equilibrium angles φ_0 and θ_0 determined from the following condition: $\partial F/\partial\varphi = \partial F/\partial\theta = 0$.

With bias of the oblong ellipsoid along the symmetry axis ($\mathbf{H}_0 \parallel \mathbf{n}$), equilibrium angle θ_0 is equal to zero at any values of field H_0, while the resonance dependence in this case is defined by the high-frequency branch of FMR:

$$\omega_{\text{res}} = \gamma(H_0 + H_{\text{KN}})$$
$$= \gamma\left[H_0 + 2K/M_0 + (3N_\perp - 4\pi)M_0\right], \quad (6)$$

where $\gamma = 1.76 \cdot 10^7\,(\text{Oe}\cdot\text{s})^{-1}$, $H_{\text{KN}} = 2K/M_0 + \Delta N M_0$ — effective anisotropy field.

With bias of the ellipsoid in the „hard“ plane $\mathbf{H}_0 \perp \mathbf{n}$ in the equilibrium state vector $\mathbf{M}_0$ lies in the plane of vectors ($\mathbf{n}$, $\mathbf{H}_0$). In this case, the equilibrium azimuth angle measured from the direction of field $\mathbf{H}_0$ (for example, from OX axis) is $\varphi_0 = 0$, and angle θ_0 is defined by the following expressions:

$$\sin\theta_0 = \begin{cases} 1, & H_0 > H_{\text{KN}} \\ \pm\dfrac{H_0}{H_{\text{KN}}}, & H_0 < H_{\text{KN}} \end{cases}. \quad (7)$$

Field dependencies of resonance frequencies for the cases in question, taking into account (1) and (5), are defined by the following expressions:

$$\omega_{\text{res}} = \begin{cases} \gamma\sqrt{H_{\text{KN}}^2 - H_0^2}, & H_0 < H_{\text{KN}} \\ \gamma\sqrt{H_0(H_0 - H_{\text{KN}})}, & H_0 > H_{\text{KN}} \end{cases}. \quad (8)$$

From (8) it follows that one of the resonance branches lies in the region of fields $H_0 < H_{\text{KN}}$, while another one is in the region of $H_0 > H_{\text{KN}}$, therefore one frequency value $\omega < \omega_0$ has two correspondent values of resonance field:

$$H_{\text{res}}^{(1,2)} = \begin{cases} \sqrt{H_{\text{KN}}^2 - \omega^2/\gamma^2} \\ \dfrac{1}{2}\left(H_{\text{KN}} + \sqrt{H_{\text{KN}}^2 + 4\omega^2/\gamma^2}\right) \end{cases}. \quad (9)$$

3. Conditions of magnetization uniformity

First, let us note the restrictions imposed on size of the particle, which MM dynamics is under consideration. Here and elsewhere, we used parameters of particle material close to those of 80Ni20Fe permalloy: $4\pi M_0 = 10^4$ Gs, $K = 10^4$ erg/cm^3, $\sigma \approx 10^{18}\,\text{s}^{-1}$, $\alpha = 0.01$, frequency of SHF-field $\omega = 2 \cdot 10^8\,\text{s}^{-1}$ and $n = 1.02$. To keep the magnetization uniformly distributed over the specimen in the presence of SHF-field, it is necessary to have maximum particle size d much less than the depth of the skin-layer $\delta = c/(2\pi\sigma\omega\mu)^{1/2}$ [18]. For above-mentioned values of parameters and $c = 3 \cdot 10^{10}$ cm/s, $\mu \approx 100$ we get $d \ll \delta \approx 10^{-4}$ cm.

The following restriction is imposed due-to the presence of thermal fluctuations, which can disturb the precession dynamics defined by the effective field acting on the MM at every instant in time. The effect of thermal fluctuations is described by exponential term $\exp(\Delta U/kT)$ [19], where $\Delta U = \Delta N^{\text{ef}} M_0^2 V/2$ — potential barrier, dividing the directions along the „easy“ axis and in the „hard“ plane, V — particle volume, $\Delta N^{\text{ef}} = H_{\text{KN}}/M_0$ — parameter of the effective anisotropy. To prevent the thermal excitation from disturbing the precession dynamics, the following condition must be met: $V > V_{\min}$ [5], where $V_{\min} = 2kT/N^{\text{ef}} M_0^2 \approx 10^{-18}\,\text{cm}^3$. Thus, for a spherical (or close to spherical) particle, it diameter $d > d_{\min} \approx 10$ nm.

One more restriction is associated with the requirement of single-domain type of the particle, which is assumed as fulfilled in the following consideration. For a single-domain particle, its radius must be less than $R_{\text{cr}} \approx \sigma_s/M_0^2$, where surface domain wall energy for permalloy is $\sigma_s \approx 1\,\text{erg/cm}^2$. Therefore, for the particle in question the following condition must be met: $d < 2R_{\text{cr}} \approx 30$ nm. According to performed estimates, optimum particle size to observe FMR is $10 < d < 30$ nm. However, it should be noted that according to [20] metal cylindrical particles with a diameter of $d \approx 40-50$ nm and a height of $h \approx 45$ nm should be considered as single-domain.

4. Numerical analysis

Fig. 1 (a, b) shows field dependencies of equilibrium angle θ_0 and resonance frequencies built using formulae (6–8). The dependence of $\theta_0(H_0)$ shows that in the region of $H_0 \geq H_{KN}$ there is one equilibrium orientation of magnetization ($\theta_0 = \pi/2$, $\mathbf{M} \parallel \mathbf{H}_0$), while in the region of $H_0 < H_{KN}$ magnetization of the ellipsoid has two symmetrical angular equilibrium positions. If bias field values are close to H_{KN}, then the angular distance between two symmetrical equilibrium positions is small as well, and can be overcome easily under the impact of a high-frequency field. With decrease in frequency the resonance fields become close to each other and at $\omega \to 0$ both branches converge in the point of $H_0 = H_{KN}$.

The dynamic equations were solved numerically based on the Runge–Kutta method. Here and elsewhere, we used parameters of particle material close to those of 80Ni20Fe permalloy ($4\pi M_0 = 10^4$ Gs, $K = 10^4$ erg/cm^3, $\alpha = 0.01$, $n = 1.02$), frequency of SHF-field $\omega = 2 \cdot 10^8\,\mathrm{s}^{-1}$, parameters of the static field were selected close to the resonance values at the specified conditions of bias and excitation. Time dependence of the excitation field is defined in the following form: $h(t) = h \sin \omega t$, where $h = 0.2$ Oe, which assumes linear character of the FMR, provided that $h \ll H_0$. With bias of the oblong ellipsoid along the axis of symmetry ($\mathbf{H}_0 \parallel \mathbf{n}$) and excitation by field $\mathbf{h} \perp \mathbf{H}_0$, the precession trajectory of vector $\mathbf{M}$ outgoes from the initial position of $\varphi_0 = \theta_0 = 0$ to the circular trajectory, which is shown in Fig. 2 on the plane (μ_x, μ_y), where $\mu_\alpha = M_\alpha/M_0$.

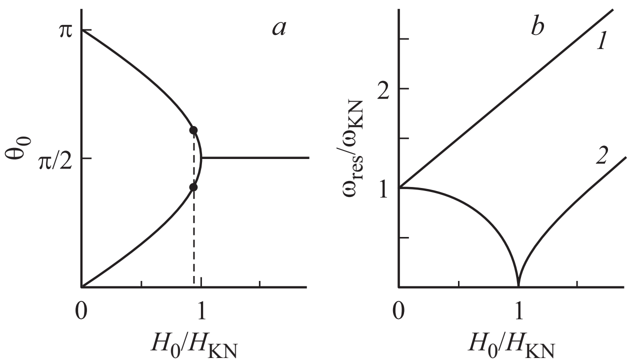

Figure 1. Field dependencies a) of equilibrium angle θ_0 and b) resonance frequency under bias of the oblong ellipsoid in the „hard“ plane (curve *2*), curve *1* — bias along the „easy“ axis.

With bias in the „hard“ plane ($\mathbf{H}_0 \perp \mathbf{n}$) the precession trajectory becomes more complicated, and its shape can be significantly affected by both value and frequency of the static field and amplitude and orientation of the varying field. The traditional implementation of FMR is correspondent to the case of orthogonal static $\mathbf{H}_0$ and high-frequency $\mathbf{h}$ fields [4]. In the following, we consider the magnetization precession of ellipsoid under a longitudinal excitation ($\mathbf{h} \parallel \mathbf{H}_0 \parallel OX$) and a weak high-frequency field ($h \ll H_0$). In this case free energy has the following form:

$$F = -M(H_0 + h \sin \omega t) \cos \varphi \sin \theta + K \sin^2 \theta + \frac{M^2}{6}\left[4\pi + (3\sin^2\theta - 2)\Delta N\right]. \tag{10}$$

Fig. 3 shows projections of precession trajectories of vector $\boldsymbol{\mu}$ on the ZOY plane built for several values of H_0 close to resonance from the moment of field switch-on until substantially stationary motion is established. At a selected frequency, in accordance with (9) resonance values of the field are $\mathbf{H}_{\mathrm{res}} = (103.45, 105.35)$ Oe. The first value corresponds to the case of $H_0 < H_{KN}$, when the direction of equilibrium vector $\mathbf{M}_0$ does not coincide with $\mathbf{H}_0$. At

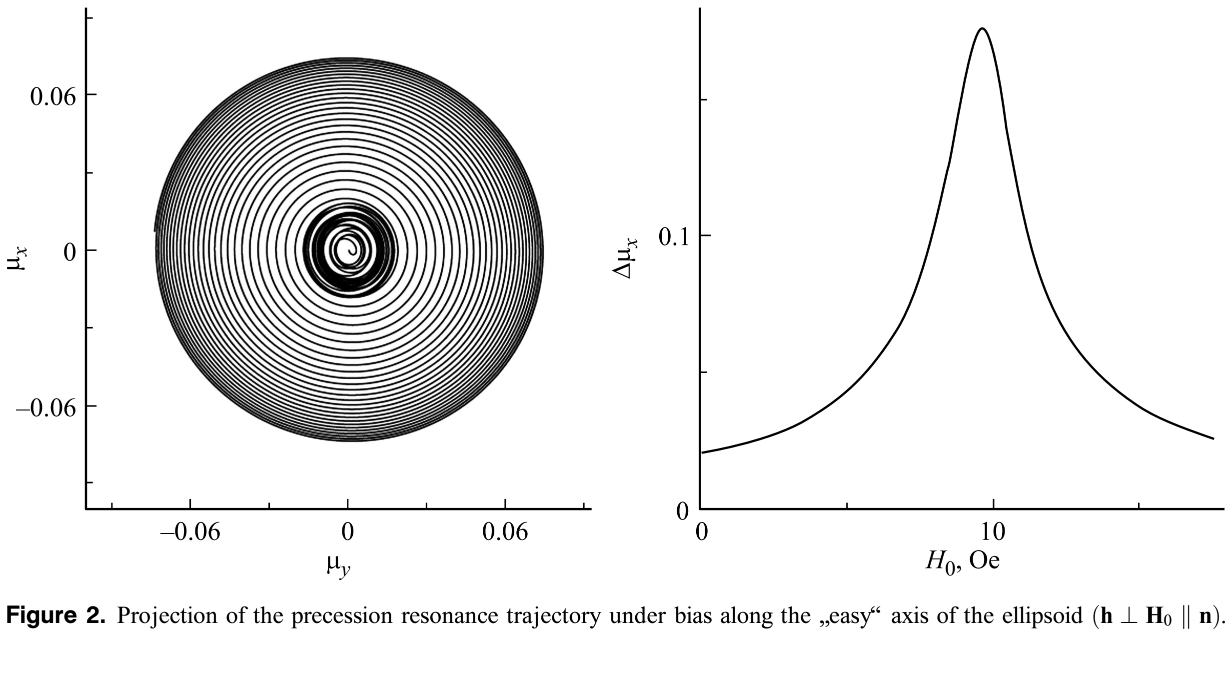

Figure 2. Projection of the precession resonance trajectory under bias along the „easy“ axis of the ellipsoid ($\mathbf{h} \perp \mathbf{H}_0 \parallel \mathbf{n}$).

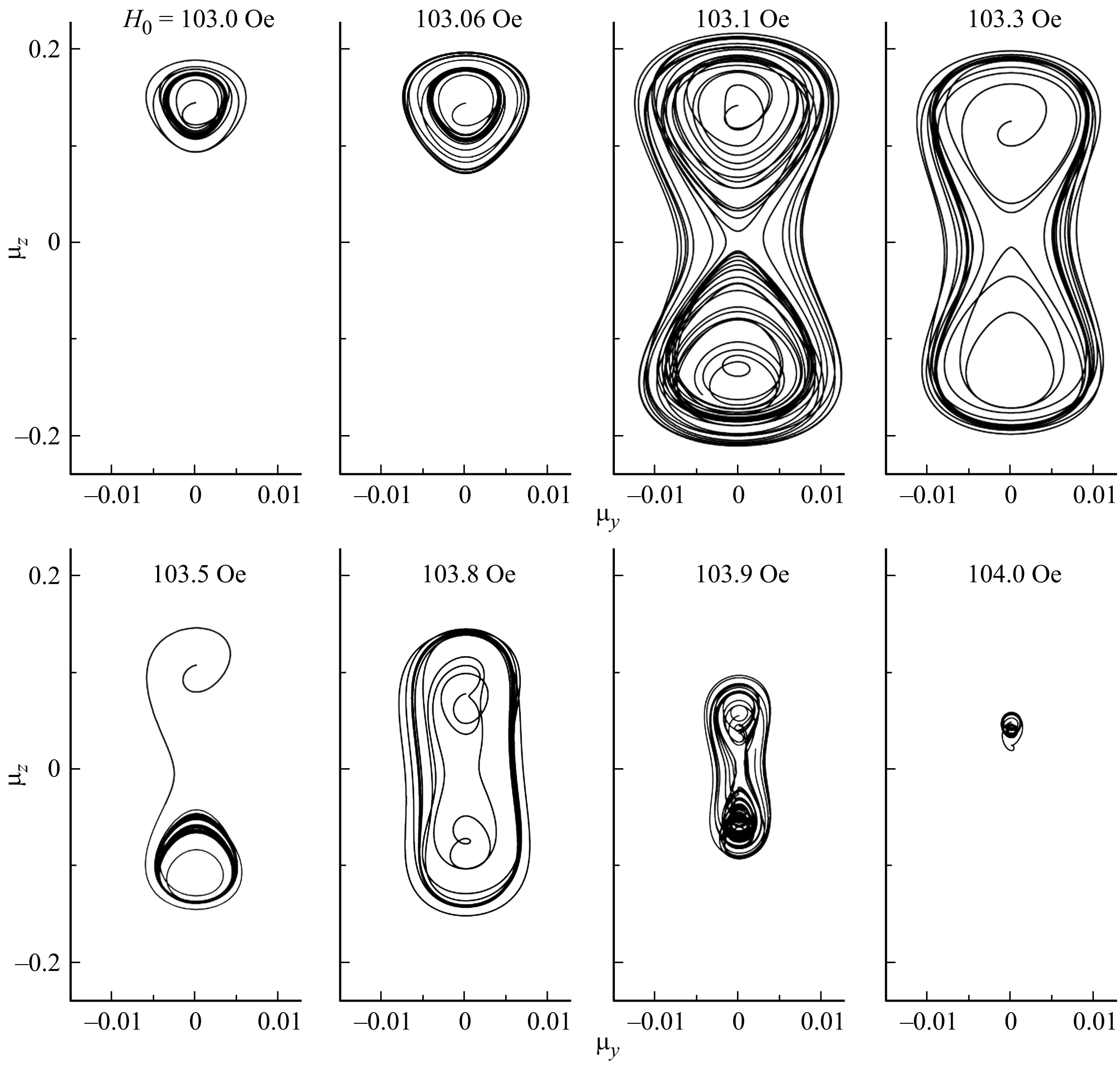

Figure 3. Projections of precession trajectories on the *ZOY* plane at various bias fields in the „hard" plane of the ellipsoid and longitudinal excitation ($\mathbf{h} \parallel \mathbf{H}_0$).

$H_0 = H_{\mathrm{KN}} = 104.116$ Oe vector $\mathbf{M}_0$ becomes parallel to field $\mathbf{H}_0$.

It can be seen from the trajectories shown in the figure that with increase in the field H_0 first a sharp increase in amplitude of the precession is observed and maximum of the response is achieved at $H_0 = 103.1$ Oe. Then, within a small interval of field $\Delta H_0 \approx 1$ Oe, along with changes in character, a decrease in amplitude of trajectories takes place, and at a field of $H_0 \simeq 104$ Oe the amplitude drops dramatically almost down to zero. It should be noted that in a narrow region of field near $H_0 \simeq 103.5$ Oe instability is manifested, which consists in change of the trajectory character: the precession starts from one equilibrium position, and the steady trajectory becomes „attracted" by the symmetric (about the „hard" plane) equilibrium position. At the same time the amplitude of this precession is considerably less than the amplitude of the precession near two equilibrium positions.

At $H_0 \geq H_{\mathrm{KN}}$, the precession under the action of longitudinal excitation field disappears. Thus, the high-amplitude precession of magnetization near the resonance static field under a weak longitudinal excitation is related to small deviations of the equilibrium magnetization from the direction of static field and the presence of a small component of magnetization normal to the SHF field when $H_0 < H_{\mathrm{KN}}$.

Fig. 4 shows two more projections of vector $\boldsymbol{\mu}$ for the field $H_0 = 103.1$ Oe, along with the spatial view of the precession trajectory with maximum amplitude under bias in the „hard" plane and a longitudinal excitation (one more projection of this trajectory is shown in Fig. 3). In contrast to the flat trajectory under bias along the „easy" axis (Fig. 2), in the case under consideration the steady trajectory is more complicated volumetric closed curve.

In this case, the change in longitudinal component μ_z for the trajectory in question is more than an order

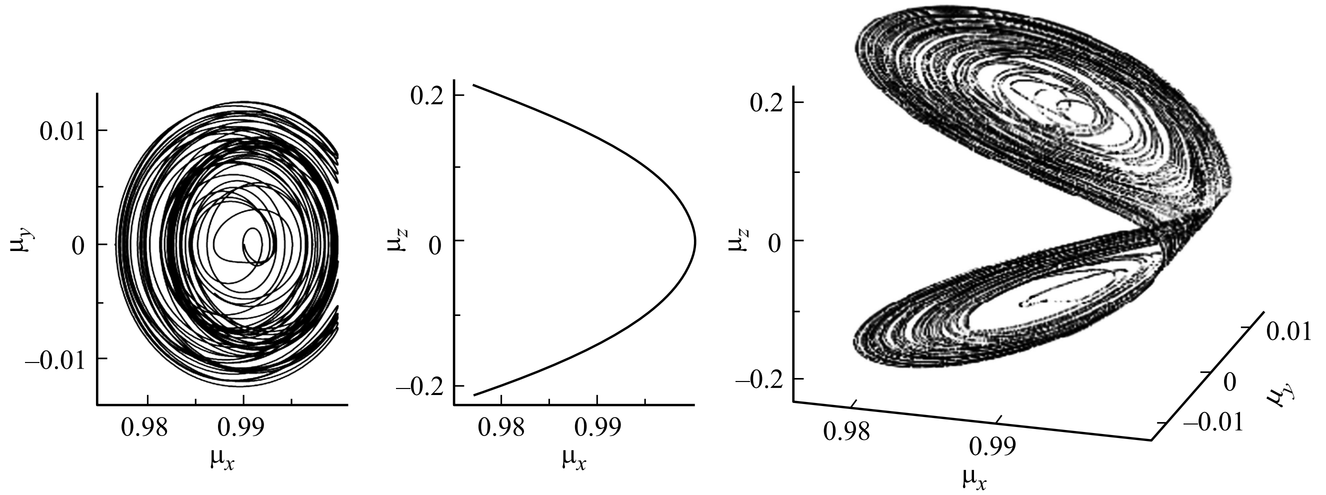

Figure 4. Two projections and general view of the resonance trajectory under bias in the „hard" plane and longitudinal excitation ($\mathbf{h} \parallel \mathbf{H}_0 \perp \mathbf{n}$).

of magnitude higher than the change in two transverse components.

It is known that response of a magnetic system for the impact of varying field is defined by the imaginary component of high-frequency susceptibility χ'', which is related to the absorbed power of SHF-field by the following relationship: $P = \chi''\omega h^2 V/2$, where V — volume of the specimen. Since frequency, amplitude of the field, as well as volume of the specimen are considered pre-defined, then the high-frequency response defined by a value of χ'' with a reasonable degree of accuracy can be linked with $\Delta\mu_z = |\mu_z^{\max} - \mu_z^{\min}|$.

With this consideration in mind, Fig. 5 illustrates the field dependence of oblong ellipsoid value under its bias in the „hard" plane for two excitation options — longitudinal and transverse (solid and dashed lines). These dependences are different in terms of number of „resonance" peaks: at the traditional (for linear FMR) transverse excitation there are two such peaks, while at the longitudinal excitation there is one peak. When approaching to the bistability field H_b, which value is defined by parameters of the particle and the excitation field (in the case under consideration $H_b = 103.1$ Oe), a sharp growth of $\Delta\mu_z$ takes place with achievement of the maximum response value. As was already mentioned, this maximum is due to the bistability, which is related to two equilibrium positions close in their angles in the region of $H_0 < H_{\mathrm{KN}}$. These positions „attract" the magnetic moment at any orientation of field $\mathbf{h}(t)$, the precession of the magnetic moment takes place near each of them with different probability (depending on proximity of the static field to H_b). Then, with increase in the field an asymmetric drop of the response takes place, which decreases abruptly almost down to zero at $H_0 \simeq 104$ Oe, which means absence of precession.

Similar behavior of the response in the region of $H_0 < H_{\mathrm{KN}}$ is observed under a transverse excitation as well

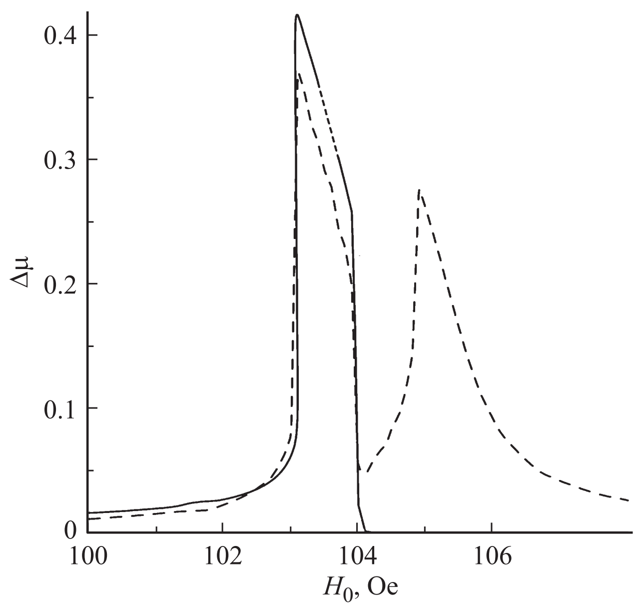

Figure 5. FMR spectrum of the oblong ellipsoid under bias in the „hard" plane, longitudinal and transverse excitation (solid and dashed lines).

(dashed line). However, in this case the response amplitude is less than in the case of longitudinal excitation, and also, in addition to the above-mentioned peak, there is a peak in the spectrum in the region of $H_0 > H_{\mathrm{KN}}$. Its amplitude is less than the amplitude of the first peak. Also, it's worth to note that the response amplitude at bias in the „hard" plane is considerably higher than the response amplitude at bias along the symmetry axis of the ellipsoid. At the same time, width of resonance peaks $\Delta H_0 \simeq 1$ Oe, which is considerably ńarrower than width of the resonance line at bias long the „easy" axis (see. Fig. 2, *b*).

5. Conclusion

The performed analysis shows that in the FMR spectrum of a single-domain uniaxial magnetic micro- or nano-particle shaped in the form of an oblong ellipsoid of revolution, with bias in the „hard“ plane and longitudinal excitation by a weak SHF-field ($\mathbf{h} \parallel \mathbf{H}_0 \perp \mathbf{n}$) in the region of $H_0 < H_{\mathrm{KN}}$ a resonance peak is observed, which position does not correspond to the resonance value of the field $H_{\mathrm{res}}^{(1)}$, amplitude is higher than that of the resonance peak under transverse excitation, and precession trajectory of magnetization has a complicated volumetric character with two „centers of attraction“. Width of this peak is considerably ńarrower than that of the resonance curve under transverse excitation. The emergence of such a peak and bistability is related to the presence of two equilibrium positions of the ellipsoid magnetic moment, which are close to each other in their angles. Peaks of similar type should also manifest in FMR spectra of oblate ellipsoid particles and in structures with cubic crystal anisotropy. Observation of similar peaks in resonance investigations of thin magnetic films and their interpretation was reported in [13,14].

Conflict of interest

The authors declare that they have no conflict of interest.

References

[1] E.Z. Meilikhov, R.M. Farzetdinova. JMMM **268**, *1–2*, 237 (2004).
[2] R.B. Morgunov, A.I. Dmitriyev, G.I. Dzhardimaliyeva, A.D. Pomogaylo, A.S. Rosenberg, Y. Tanimoto, M. Leonowicz, E. Sowka. Physics of the Solid State **49**, *8*, 1436 (2007) (in Russian).
[3] A. Sukhov, J. Berakdar. Phys. Rev. B **79**, *13*, 134433 (2009).
[4] Yu.I. Dzhezherya, K.O. Demishev, V.N. Korenivsky. Journal of Experimental and Theoretical Physics **142**, *2* (*7*), 8 (318). (in Russian).
[5] Ye.Z. Meylikhov, R.M. Farzetdinova. Physics of the Solid State **56**, *12*, 2329 (2014) (in Russian).
[6] A.M. Shutyi, D.I. Sementsov. Letters to the Journal of Experimental and Theoretical Physics **99**, *12*, 806 (2014) (in Russian).
[7] A.M. Shutyĭ, S.V. Eliseeva, D.I. Sementsov. Phys. Rev. B **91**, *2*, 024421 (2015).
[8] T. Kiseleva, S. Zholudev, A. Novakova, T. Grigoryeva. Compos. Struct. **138**, 12 (2016).
[9] I.S. Poperechny, Yu.L. Raikher. Phys. Rev. B **93**, *1*, 014441 (2016).
[10] Ferromagnetic resonance. Collected papers / Ed. by S.V. Vonsovsky, Fizmatlit, M. (1961) (in Russian).
[11] A.G. Gurevich, G.A. Melkov. Magnetic oscillations and waves, Nauka, M. (1994) (in Russian).
[12] V.G. Shavrov, V.I. Shcheglov. Magnetization dynamics in conditions of its orientation change, Fizmatlit, M. (2019) (in Russian).
[13] B.A. Belyaev, A.V. Izotov, S.Ya. Kiparisov. Letters to the Journal of Experimental and Theoretical Physics **74**, *4*, 248 (2002) (in Russian).
[14] T.M. Vasilevskaya, D.I. Sementsov. Letters to the Journal of Experimental and Theoretical Physics **137**, *5*, 861 (2010) (in Russian).
[15] M.A. Shamsutdinov, L.A. Kalyakin, A.T. Kharisov. Journal of Technical Physics **80**, *6*, 106 (2010) (in Russian).
[16] P.E. Zil'berman, A.G. Temiryazev, M.P. Tikhomirova. Journal of Experimental and Theoretical Physics **108**, *1* (*7*), 7 (281). (in Russian)
[17] V.V. Tikhonov, A.V. Tolkachev. Physics of the Solid State **36**, *1*, 185 (1994) (in Russian).
[18] L.D. Landau, E.M. Lifshitz. Theoretical physics Nauka, M. (1982). V. VIII. (in Russian)
[19] L. Neel. Ann. Geophys. (C.N.R.S.) **5**, 99 (1949).
[20] S.A. Nepiyko. Physical properties of small metal particles, Nauk. dumka, Kiev (1985) (in Russian).